Synthesis of $H_2V_3O_8$ Single-Crystal Nanobelts

Gui-cun Li,*[a,b] Shu-ping Pang,[b] Zhao-bo Wang,[b] Hong-rui Peng,[b] and Zhi-kun Zhang*[a,b]

Keywords: Vanadium / Layered compounds / Nanobelts / Nanostructures

Orthorhombic $H_2V_3O_8$ single-crystal nanobelts with a thickness of less than 30 nm and a length up to several hundreds of micrometers have been synthesized using bulky divanadium pentoxide powders as a precursor. The synthetic process is free of any templates and reducing agents. Divanadium pentoxide undergoes a redox reaction under hydrothermal conditions. The influences of pH, reaction time, and temperature on the morphologies of the resulting products have been investigated. The belt-like $H_2V_3O_8$ with a high surface area may be beneficial to lithium insertion between the V_3O_8 layers for application in batteries.

Introduction

In recent years, there has been increased interest in synthesizing one-dimensional (1D) nanostructures of vanadium oxides and their derivative compounds, such as nanorod, nanowires, nanotubes, nanobelts, and nanoribbons, because of their diverse physicochemical properties and potential applications including use as cathode materials for lithium batteries,[1] and as electric field-effect transistors.[2,3] Among them, the belt-shaped 1D nanostructures are expected to represent important building blocks for nanodevices.[4,5] Vanadium oxide hydrate ($H_2V_3O_8$), one of the vanadium oxyhydroxides containing V^{5+} and V^{4+} in a ratio of 2 to 1,[6] is of interest because of its layered structure and redox activity. Considerable efforts have been made on the synthesis of 1D nanostructures of vanadium oxide and their derivative compounds. For example, Pinna et al.[7,8] synthesized divanadium pentoxide nanorods and nanowires by a colloidal self-assembly made up of sodium bis(2-ethylhexyl)sulfosuccinate Na(AOT)/isooctane/H_2O. Nesper et al.[9] used neutral surfactant molecules such as primary aliphatic amines, together with vanadium alkoxide precursors to generate redox-active vanadium oxide nanotubes. Yu et al.[10] reported the synthesis of multicomponent $Na_2V_6O_{16}\cdot 3H_2O$ single-crystal nanobelts in the presence of F^- ions, however, without F^- ions or in the presence of other anions such as Cl^-, Br^-, NO_3^-, and SO_4^{2-}, nanobelts could not be obtained. Qian et al.[11] prepared single-crystal $VO_x\cdot nH_2O$ nanoribbons relying on the presence of polyethylene glycol 400, but the values of x and n are uncontrolled. Li et al.[12] reported that metastable vanadium dioxide single-crystal nanobelts were synthesized by hydrothermal synthesis using formic acid as the reducing agent. However, the synthesis of pure $H_2V_3O_8$ 1D nanostructures remains challenging to material scientists. In this paper, we report a low-cost and simple approach for the synthesis of $H_2V_3O_8$ single-crystal nanobelts by hydrothermal processing of bulky divanadium pentoxide (V_2O_5) powders in hydrochloric acid solution without the aid of any templates or reducing agents.

Results and Discussion

XRD patterns of the V_2O_5 precursor and $H_2V_3O_8$ nanobelts are shown in parts A, B of Figure 1, respectively. All the peaks in Figure 1 (see A) can be indexed to the orthorhombic crystalline phase of V_2O_5 in agreement with literature values (JCPDS 89–0612). After hydrothermal treatment, a pure orthorhombic crystalline phase of $H_2V_3O_8$ [space group: *Pnam*] (see B in Figure 1) with calculated lattice contents a = 16.99 Å, b = 9.40 Å, c = 3.64 Å, was obtained, which is consistent with literature values (JCPDS 85–2401). From the structural data, it is expected that the ratio of V^{5+} and V^{4+} in the product is 2 to 1, indicating that V^{5+} is reduced partly to V^{4+}.

Figure 2 shows SEM images of $H_2V_3O_8$ nanobelts synthesized at pH 4. Lower magnification SEM images (see A in Figure 2 and in the Supporting Information Figure 1S) reveal that the precipitates consist of a large quantity of uniform 1D nanostructures with typical lengths in the range of several tens to several hundreds of micrometers. The long fibrillar morphologies can even be seen with the naked eye. A magnified SEM image (B in Figure 2) indicates that the

[a] Fishery College, Ocean University of China, Shandong, Qingdao 266003, P. R. China
[b] Key Laboratory of Nanostructured Materials, Qingdao University of Science and Technology, Shandong, Qingdao 266042, P. R. China
Fax: +86-532-402-2869
E-mail: guicunli@qust.edu.cn
Supporting information for this article is available on the WWW under http://www.eurjic.org or from the author.

  DOI: 10.1002/ejic.200400967

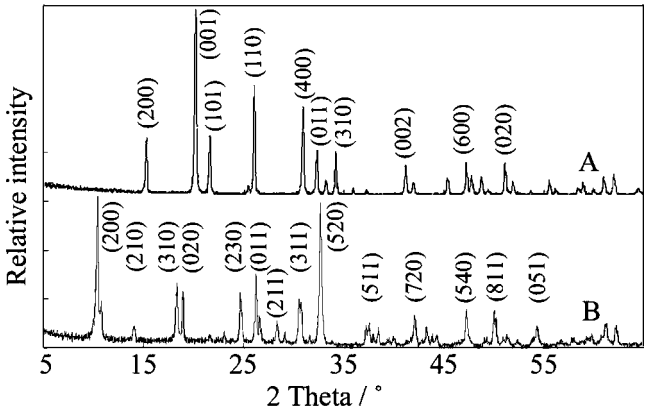

Figure 1. XRD patterns of the initial V_2O_5 precursor (A) and $H_2V_3O_8$ nanobelts synthesized at pH 4 (B).

geometrical shape of the $H_2V_3O_8$ nanostructures is a belt. The ends of these nanobelts are irregular. The typical thickness and width are less than 30 nm and 100–300 nm, respectively. In addition, some nanobelts have terraces of the different $H_2V_3O_8$ layers, indicating that some of the nanobelts stick together. The cleaved $H_2V_3O_8$ layers are clearly visible as indicated by an arrow in Figure 2 (C), so it can be inferred that the belt-like materials may be derived from the cleavage of $H_2V_3O_8$ layers in the reaction process. A typical TEM image of $H_2V_3O_8$ nanobelts is presented in Figure 2 (D). The width is consistent with SEM images (B in Figure 2). The ripple-like strain contrast can also be seen clearly in $H_2V_3O_8$ nanobelts. The selected area electron diffraction (SAED) pattern (E in Figure 2) taken from a single nanobelt indicated that the nanobelts are single crystals and the growth occurs along the [001] direction. The HRTEM image (F in Figure 2) shows the clearly-resolved interplaner distances d_{011} = 0.339 nm and d_{020} = 0.468 nm, which further confirms the growth direction of the nanobelts. The $H_2V_3O_8$ nanobelts are constructed from both VO_6 octahedra and VO_5 trigonal bipyramids. Two VO_6 octahedra are piled up along the *c* axis by sharing edges, which are connected by two-shared VO_5 trigonal bipyramids along the *b* axis, and then a V_3O_8 layer along the *a* axis is formed.[6] The layered structures composed of V_3O_8 layers seem to favor insertion and deinsertion of lithium for application in batteries.[13,14]

The pH value, reaction time, and temperature are important factors for the formation of $H_2V_3O_8$ nanobelts. The width of $H_2V_3O_8$ nanobelts can be controlled by adjusting the pH value. At pH 5, nanobelts with a width of 1 μm are obtained as shown in Figure 3 (A). The nanobelts can be folded without fracture, indicating that their flexibility is very high. At pH 3, the width of the nanobelts in Figure 3 (B) decreased to 90–110 nm. The reaction can proceed without the addition of any hydrochloric acid, but the reaction rate is very slow. It is found that the reaction rate increases when pH values decrease from 7 to 3 possibly because of the formation of various polyvanadate ions at different pH values in aqueous solution. When the reaction is carried out at pH 4 for 6 h, little green product is generated because of

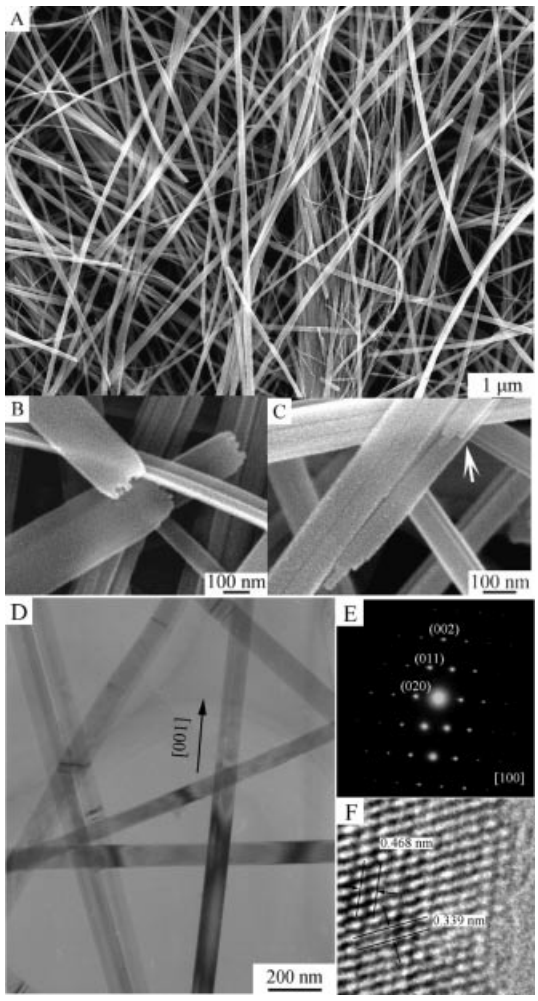

Figure 2. SEM (A, B, and C), TEM (D), and HRTEM (F) images of $H_2V_3O_8$ nanobelts synthesized at pH 4. Figure 2E shows the SAED pattern taken from a single nanobelt.

the inefficient reduction. With an increased reaction time, the color of the product changes from yellow to green. After hydrothermal treatment at pH 4 at 160 °C for 24 h, the reduction is also incomplete, so the nanobelts coexist with particles in the product (see Supporting Information, Figure 2S).

Figure 4 (A, B) present UV/Vis spectra of the initial V_2O_5 precursor and $H_2V_3O_8$ nanobelts synthesized at pH 4, respectively. Part B of Figure 4 shows a broad adsorption peak centered around 850 nm and a weak shoulder around 630 nm, corresponding to the *d–d* electronic transitions of V^{4+} in $H_2V_3O_8$ nanobelts,[15–17] so the product is green. In comparison with Figure 4 (A), the intensity of the adsorption peak of V^{4+} increases greatly, indicating the reduction of V^{5+} to V^{4+} during the course of hydrothermal treatment.

The reaction was carried out in the absence of any reducing agent, so V_2O_5 may undergo a redox reaction under hydrothermal conditions and it is difficult to completely reduce V_2O_5 to VO_2. The basic reaction process for the synthesis of $H_2V_3O_8$ nanobelts may be expressed as follows:

$$6\,V_2O_5 + 4\,H_2O \rightleftharpoons 4\,H_2V_3O_8 + O_2$$

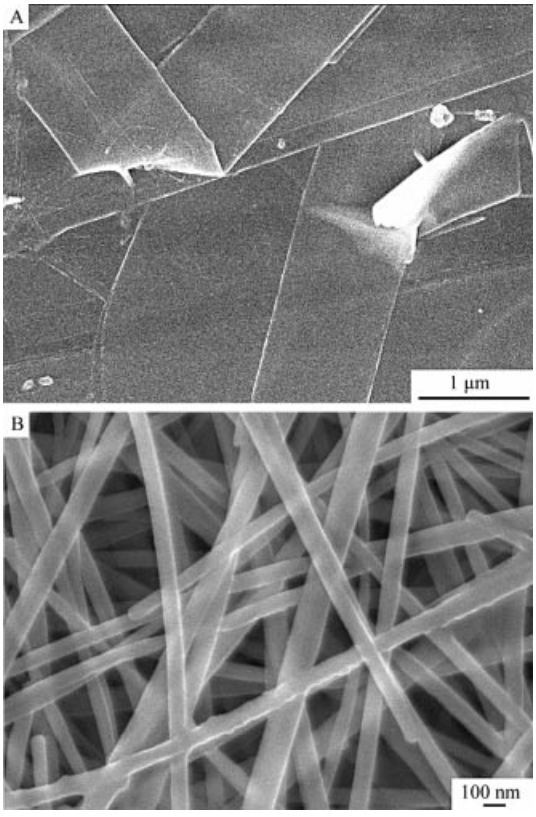

Figure 3. SEM images of $H_2V_3O_8$ nanobelts synthesized with different pH values. (A) at pH 5, (B) at pH 3.

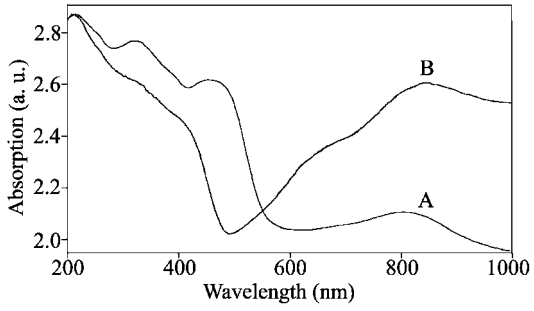

Figure 4. UV/Vis spectra of the initial V_2O_5 precursor (A), and $H_2V_3O_8$ nanobelts synthesized at pH 4 (B).

The redox reaction process is free of any templates and surfactants, so it is supposed that the formation of the belt-like $H_2V_3O_8$ is probably related to the layered structure of $H_2V_3O_8$. V_2O_5 partly dissolves in water to produce various polyvanadate ions at different pH values in aqueous solution, which can undergo a redox reaction to form $H_2V_3O_8$ clusters under hydrothermal conditions. Then, the $H_2V_3O_8$ clusters serve as the sites for the heterogeneous nucleation of the nanobelts, which subsequently crystallize along the [001] direction of $H_2V_3O_8$ single crystals and grow in belt-like structures through a topotactic transformation mechanism.

Conclusions

In conclusion, we have demonstrated a facile route to the synthesis of $H_2V_3O_8$ nanobelts. The synthetic process is free of any templates and reducing agents. The thickness and length of $H_2V_3O_8$ nanobelts are less than 30 nm, and up to several hundreds of micrometers, respectively. The width of $H_2V_3O_8$ nanobelts can be controlled by adjusting the pH values. The belt-like $H_2V_3O_8$ with a high surface area may be beneficial to lithium insertion between the V_3O_8 layers for application in batteries.

Experimental Section

An optimized procedure for the synthesis of $H_2V_3O_8$ single-crystal nanobelts is described as follows: V_2O_5 powder (0.15 g) was dispersed into distilled water (40 mL). Then, an appropriate amount of hydrochloric acid was added dropwise to the orange mixture to adjust pH values in the range of 3–5. The slurry solution was placed in a 50-mL autoclave with a Teflon liner after ultrasonic vibration for 10 min. The autoclave was maintained at 190 °C for 24 h and then air cooled to room temperature. The green precipitate was collected and washed with distilled water and anhydrous alcohol several times, and then dried in vacuo at 60 °C for 10 h. The yield of the $H_2V_3O_8$ nanobelts is estimated to be higher than 90%.

The crystal structures of the initial V_2O_5 precursor and the resulting product were characterized by an X-ray diffractometer (Rigaku D-max-γA XRD with Cu-K_α radiation, λ = 1.54178 Å). The morphologies and sizes of the resulting products were observed by field-emission scanning electron microscopy (FE-SEM, JSM 6700F) and high-resolution transmission electron microscopy (HRTEM, JEOL 2010), respectively. The optical properties of the initial V_2O_5 precursor and the resulting product were determined by UV/Vis spectroscopy (Cary 500 UV/Vis-NIR spectrophotometer).

Supporting Information Available: Figure 1S, lower magnified SEM image of $H_2V_3O_8$ nanobelts synthesized at pH 4 at 190 °C for 24 h. Figure 2S, SEM image of the product obtained at pH 4 at 160 °C for 24 h.

Acknowledgments

This project is partly supported by the National Center for Nanoscience and Technology, P. R. China.

[1] A. Dobley, K. Ngala, S. Yang, P. Y. Zavalij, M. S. Whittingham, *Chem. Mater.* **2001**, *13*, 4382–4386.
[2] G. T. Kim, J. Muster, V. Krstic, J. G. Park, Y. W. Park, S. Roth, M. Burghard, *Appl. Phys. Lett.* **2000**, *76*, 1875–1877.
[3] J. Muster, G. T. Kim, V. Krstić, J. G. Park, Y. W. Park, S. Roth, M. Burghard, *Adv. Mater.* **2000**, *12*, 420–424.
[4] Z. W. Pan, Z. R. Dai, Z. L.Wang, *Science* **2001**, *291*, 1947–1949.
[5] E. Comini, G. Faglia, G. Sberveglieri, Z. W. Pan, Z. L.Wang, *Appl. Phys. Lett.* **2002**, *81*, 1869–1871.
[6] Y. Oka, T. Yao, N. Yamamoto, *J. Solid State Chem.* **1990**, *89*, 372–377.
[7] N. Pinna, U. Wild, J. Urban, R. Schlögl, *Adv. Mater.* **2003**, *15*, 329–331.

[8] N. Pinna, M. Willinger, K. Weiss, J. Urban, R. Schlögl, *Nano Lett.* **2003**, *3*, 1131–1134.
[9] M. E. Spahr, P. Bitterli, R. Nesper, M. Müller, F. Krumeich, H. U. Nissen, *Angew. Chem., Int. Ed. Engl.* **1998**, *37*, 1263–1265.
[10] J. Yu, J. C. Yu, W. Ho, L. Wu, X. Wang, *J. Am. Chem. Soc.* **2004**, *126*, 3422–3423.
[11] L. Kong, Z. Liu, M. Shao, Q. Xie, W. Yu, Y. Qian, *J. Solid State Chem.* **2004**, *177*, 690–695.
[12] J. Liu, Q. Li, T. Wang, D. Yu, Y. Li, *Angew. Chem., Int. Ed. Engl.* **2004**, *43*, 5048–5052.
[13] V. Legagneur, A. L. G. L. Salle, A. Verbaere, A. Piffard, D. Guyomard, *Electrochim. Acta* **2002**, *47*, 1153–1161.
[14] V. Legagneur, A. L. G. L. Salle, A. Verbaere, A. Piffard, D. Guyomard, *J. Mater. Chem.* **2000**, *10*, 2805–2810.
[15] K. Takahashi, S. J. Limmer, Y. Wang, G. Cao, *J. Phys. Chem. B* **2004**, *108*, 9795–9800.
[16] E. L. Crepaldi, D. Grosso, G. J. A. A. Soler-Illia, P. A. Albouy, H. Amenitsch, C. Sanchez, *Chem. Mater.* **2002**, *14*, 3316–3325.
[17] X. Gao, M. A. Banares, I. E. Wachs, *J. Catal.* **1999**, *188*, 325–331.

Received: November 21, 2004

